INTERNATIONAL JOURNAL OF INTEGRATED ENGINEERING
ISSN: 2229-838X e-ISSN: 2600-7916

IJIE

Vol. 17 No. 9 (2025) 420-433
https://publisher.uthm.edu.my/ojs/index.php/ijie

Climate Change Impacts on Future Rainfall in Padas River Basin, Sabah, Malaysia Using Statistical Downscaling Method

Sazali Othman[1], Muhammad Syukri Mohamed Rodzi[1], Foo Huat Lim[2], Siti Nazahiyah Rahmat[3], Nurul Nadrah Aqilah Tukimat[4]*, Wan Zunairah Othman[4], Muhammad Hanafi[3]

[1] *Department of Irrigation and Drainage, Persiaran Rimba Permai, Cyber 8, 63000 Cyberjaya, Selangor, MALAYSIA*
[2] *Angkasa Consulting Services Sdn. Bhd., Subang Jaya, 47620 Selangor, MALAYSIA*
[3] *Faculty of Civil Engineering and Built Environment, Universiti Tun Hussein Onn Malaysia (UTHM), 86400 Parit Raja, Batu Pahat, Johor, MALAYSIA*
[4] *Faculty of Civil Engineering Technology, Universiti Malaysia Pahang Al-Sultan Abdullah (UMPSA), 26300 Gambang, Pahang, MALAYSIA*

*Corresponding Author: nadrah@umpsa.edu.my
DOI: https://doi.org/10.30880/ijie.2025.17.09.029

Article Info

Received: 13 May 2025
Accepted: 5 December 2025
Available online: 31 December 2025

Keywords

Climate projection, CMIP6, Padas River Basin, statistical downscaling

Abstract

The objective of this study was to assess the influence of climate change on the rainfall across the Padas River Basin, Sabah, Malaysia. Observed rainfall data (1985–2014) and downscaled climate model outputs (2025–2100) from four of the most suitable Global Climate Models (GCMs) (CMCC-CM2, IPSL-CM6A, MIROC6 and MRI-ESM2) were employed. The projected rainfall trend was analysed based on the 10th (P10), 50th (P50) and 90th (P90) percentiles to assess low, median, and high rainfall scenarios, allowing a more comprehensive understanding of uncertainty and risk in future rainfall patterns. The projection suggest an overal increase in rainfall for all months in the future, attributable to a lengthened wet season during the study period. Compared with the historical baseline, the highest monthly increase is projected in May (+60.3 mm), followed by Nov (+46.8 mm), while Feb shows the smallest increment (+5.5%). The projected increase in monthly rainfall between May and November may elevate future flood risks. Annual rainfall is expected to rise by approximately 5.4% (2025-2050) and 7.4% (2051-2100), with the highest intensity concentrated near coastal areas. Under SSP2–4.5 and SSP5-8.5, the mean annual rainfall is projected less than 3,625 mm and 4,030 mm, respectively. All four (4) models indicate a similar spatial rainfall pattern, with the northeastern part of the basin receiving more rainfall. In the long-term P90 scenario, coastal areas are projected to experience higher rainfall with cumulative rainfall less than 300,000 mm over the 76 years period. Meanwhile, the long-term P50 scenario shows results consistent with historical monthly data. These findings are essential for water management and long-term sustainability of water resources under changing climatic conditions.

1. Introduction

Information on water availability and water needs is crucial especially for water resource stressed areas. One of the most significant factors influencing the worldwide circulation of water availability under the influence of climate change is precipitation. According to the Intergovernmental Panel on Climate Change (IPCC), climate change is expected to intensify the global hydrological cycle, resulting in greater variability in precipitation patterns, with some regions experiencing more intense rainfall and others facing prolonged dry periods [1]–[4]. Recent Coupled Model Intercomparison Project Phase 6 (CMIP6)-based assessments indicate that climate change will alter precipitation patterns and intensify extremes across Southeast Asia, with substantial inter-model spread in magnitude and seasonality of changes [5], [6].

Many studies have demonstrated strong evidence of climate change on rainfall characteristics across the world including Malaysia [7]–[13]. Recent analyses using long-term rainfall records and CMIP6 projections have confirmed increasing rainfall variability and more frequent extreme events in Malaysia and neighboring countries [14]. In Sarawak, Malaysia, means annual rainfall was projected to increase in almost all parts of the state under all Representative Concentration Pathways (RCPs) with a higher increase in northern coastal region [15]. Similar findings over Borneo indicate observed and projected shifts in climate zones and precipitation extremes, with mechanisms such as Borneo vortices contributing to localized heavy rainfall [6], [16]. The vacillations of rainfall will influence the runoff and water accessibility which tends to be a major issue as the demand for consumable water increases. Hence, understanding the impact of climate change at regional and local scales is crucial to enhance planning, development and management for a climate-resilient future.

Projecting future rainfall scenarios is one step toward addressing the issues posed by climate change. In year 2016, the CMIP6 was introduced as the latest scenario set for the analyses and projections of current and future climate. CMIP6 simulation aims to broaden the understanding on how the earth system reacts to climate change signals and how future climate forcings can be assessed based on the scenarios narratives [17]. The new shared socioeconomic pathway (SSP) scenarios incorporate the socioeconomic changes along with greenhouse gas emissions to project future climates. Among the SSPs described by Riahi *et al.* [18], SSP2-4.5 and SSP5-8.5 were selected for this study because they represent a medium stabilization scenario and a high-emission scenario, respectively, which are most relevant for assessing a range of plausible future climate impacts. Other pathways, such as SSP1-2.6 and SSP3-7.0, were excluded due to limited availability of downscaled data for the study region and lower policy relevance for current planning scenarios.

Only a few studies have applied CMIP6 models to evaluate future climate impacts across various regions and sectors, demonstrating their growing importance in climate research [15]–[21]. CMIP6 GCMs different from earlier versions by providing a more accurate depiction of the Earth's physical processes and by reducing systematic bias compared with their predecessors. Therefore, this study, comprehensively assesses the possible future changes in surface climate over the Padas River Basin using the latest scenario set adopted in the IPCC Sixth Assessment Report (AR6). Although regional CMIP6 assessments have been conducted for Peninsular Malaysia and parts of Borneo [21], [22], the accuracy of CMIP6 models in simulating rainfall over the Padas River Basin has not yet been investigated. This represents a critical knowledge gap given the basin's importance for water supply and hydropower generation in Sabah. Moreover, the Government of Malaysia is developing the National Water Balance Management System (NAWABS) for major river basins. The NAWABS emphasises the need to project possible future climate scenarios to help policy makers, water authorities and related agencies prepare mitigation and adaptation plans for potential risks to water availability.

2. Methodology

2.1 Study Area and Data

The Padas River Basin lies in the southern part of Sabah, Malaysia between latitude 45°05′ and 50°50′S and longitudes 115°30′ and 116°30′E (Fig. 1). The area represents the second largest catchment in Sabah. The major area of this basin is covered by agricultural activities such as palm oil and rubber plantations, paddy and dryland crops. The total catchment area is approximately 8,774 km^2. It is made up of three major basins, the Pegalan River, Sook River and the Padas River proper. The Padas River enters a flood plain at Kuala Tomani and then continues to Tenom where the Pegalan River joins it on the right bank. After joining the Pegalan River, the Padas River turns north - west and cuts through the Crocker Range via the Tenom Gorge to Beaufort. Below Beaufort the river meanders across the Klias Peninsular before entering the sea at Brunei Bay. The Padas River Basin spreads across five districts in the lower western region of Sabah. These five districts cover a total area of 11,756 km^2, those are Tambunan District. Keningau District. Tenom District, Beaufort District, and Sipitang District.

According to historical data provided by MetMalaysia, temperature is relatively uniform throughout the year approximately 27°C, with high humidity. Northeast winds generally prevail during November-February and southwest winds during April-July. During these periods, rainfall is abundant especially during the period of

Int. Journal of Integrated Engineering Vol. 17 No. 9 (2025) p. 420-433

northeast winds. Meanwhile according to the historical data provided by Department of Irrigation and Drainage (DID, Malaysia), a trend of decreasing in rainfall volume from the coastal area of Sipitang toward the interior is obvious. To the west of the Crocker and Melingan Range, the mean annual rainfall varies from 2,500 – 4,000 mm while in the interior areas to the east of the ranges it varies from 1,500 – 2,300 mm. The central part of the Pengalan Upper Padas drainage area is shelter from the southwest winds by the Crocker range on its western boundary and from the northeast winds by the mountainous area north and northeast of the Pengalan and Sook area.

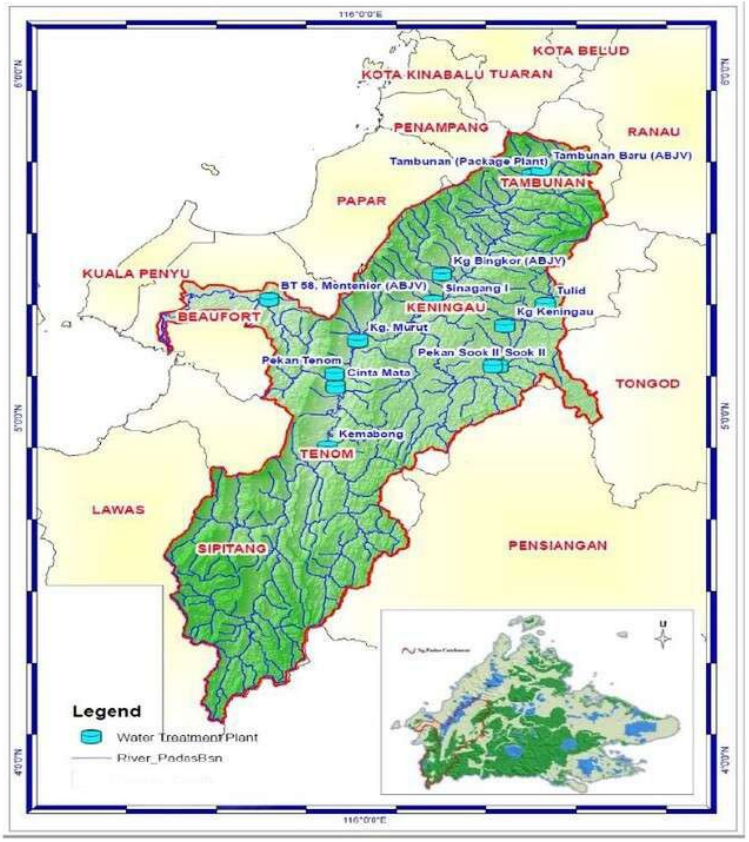

Fig. 1 *Location of Padas River Basin*

A total of 12 rainfall stations in the Padas River Basin were selected in the current study as shown in Fig. 2 and Table 1. Selection and adoption of the stations for the analysis were based on the sufficiently long records of data, e.g., records of more than 30 years are more representative of the long-term trends and recent catchment characteristics of the hydrological condition of the Padas River Basin, and reasonably good quality and reliable data. The annual rainfall is generally lower at the upper catchment with a mean of 2000 mm and highest towards the coast at about 3400 mm. Relatively low rainfalls were recorded at several stations, especially at Keningau, Batu Bajau, Tambunan, Apin-Apin and Kemabong. These stations receive less rainfall throughout the year. The Keningau catchment has the lowest average annual rainfall of 1527 mm and is the most susceptible to drought.

2.2 Missing Data Treatment Using Inverse Distance Weighted (IDW)

Missing data from the station was gap-filled using Inverse Distance Weighted (IDW) method [19]. This is to ensure the data provided is complete, homogeneous, and reliable before performing the climatic analysis. The IDW method which estimates missing value based on observed values at nearby station is shown in Equation (1).

$$V_o = \frac{\sum_{i=1}^{n}(V_i/D_i)}{\sum_{i=1}^{n}(1/D_i)} \quad (1)$$

where V_o is the assessed value of the missing data, V_i is the value of same parameter at i^{th} nearest station, D_i is the distance between the station with missing data and the i^{th} nearest station.

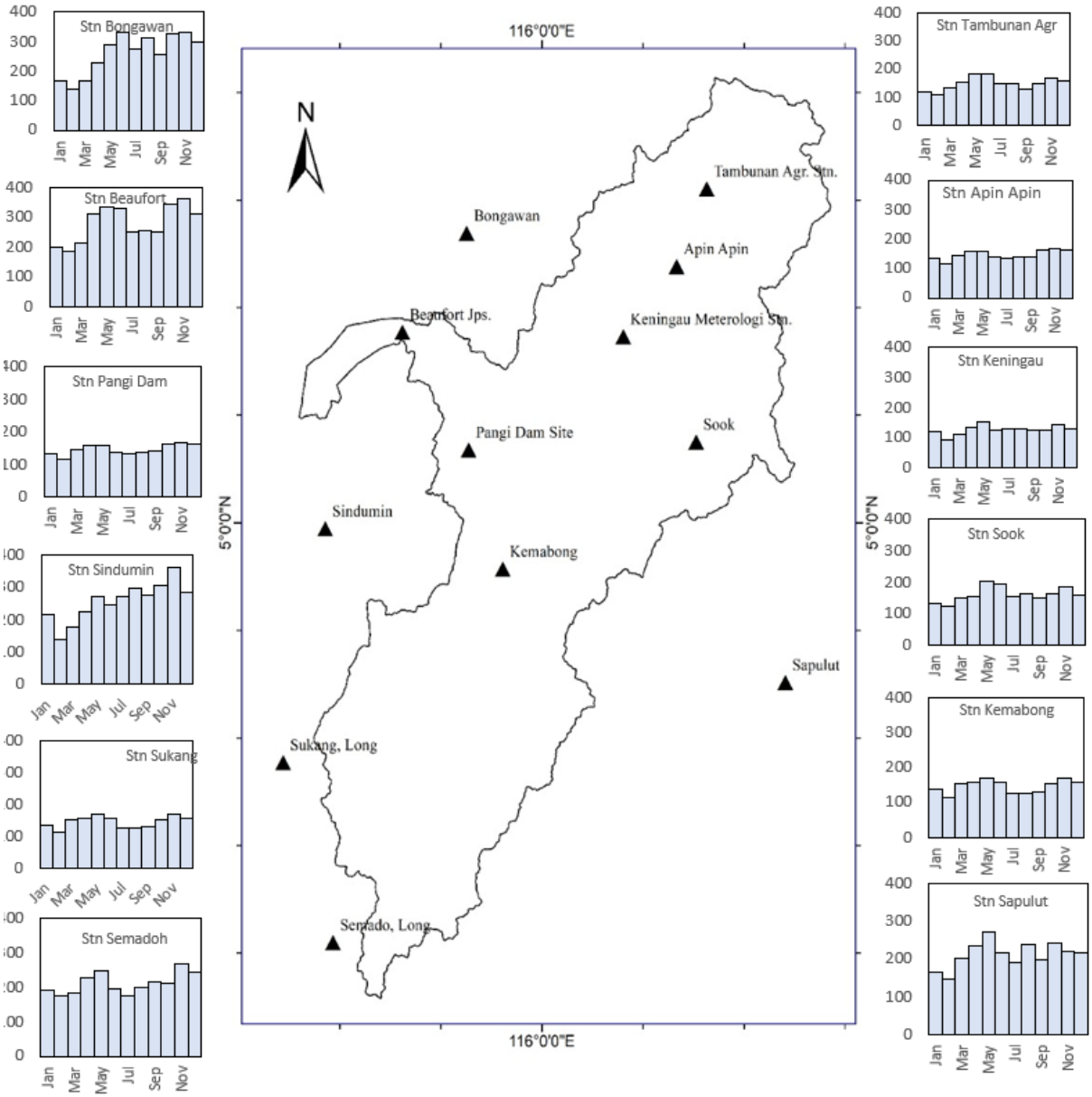

Fig. 2 *Rainfall stations in Padas River Basin*

Table 1 *List of Rainfall Stations*

No	Location	Station No.	Name of Station	Coordinate	
				Longitude	Latitude
1	Sabah	5663001	Tambunan Agr Stn	05° 37′ 15″	116° 19′ 35″
2		5462001	Apin-Apin	05° 28′ 35″	116° 16′ 00″
3		5558001	Bongawan	05° 32′ 17″	115° 51′ 03″
4		5361002	Keningau MET	05° 20′ 45″	116° 09′ 40″
5		5163002	Sook	05° 09′ 00″	116° 18′ 20″
6		5158001	Pangi Dam Site	05° 08′ 08″	115° 51′ 17″
7		5357003	Beaufort Jps	05° 21′ 15″	115° 43′ 25″
8		4955001	Sindumin	04° 59′ 20″	115° 34′ 15″
9		4764002	Sapulut	04° 42′ 10″	116° 28′ 55″
10		4959001	Kemabong	04° 54′ 50″	115° 55′ 20″
11	Sarawak	4554001	Sukang Long	04° 33′ 15″	115° 29′ 15″
12		4255006	Semado Long	04° 13′ 10″	115° 35′ 10″

Int. Journal of Integrated Engineering Vol. 17 No. 9 (2025) p. 420-433

2.3 Statistical Downscaling Method

For the climate projection, the possible future changes in the rainfall of study area were comprehensively assessed using the latest scenario, SSPs. These new socioeconomic pathway scenarios incorporate the socioeconomic changes along with greenhouse gas emissions to project future climate. The future climates were analysed under two future SSP scenarios, namely a medium forcing scenario SSP2-4.5 and a strong forcing scenario SSP5-8.5. These two pathways represent respectively a middle of the road pathway (SSP2) and a pathway with fossil-fueled development (SSP5). The monthly rainfall simulations of CMIP6 GCMs for the period of 1985–2014 were used to assess their performances. The data were downloaded from https://esgf-node.llnl.gov/projects/ cmip6/. Four (4) selected models from the CMIP6 archive are listed in Table 2.

Table 2 *IPCC's CMIP6 GCMs used in the study*

Assessment Report (ARs)	Model	Modelling Institutions	Spatial Resolution	References
AR6 (SSP2-4.5 and SSP8.5)	MRI-ESM2-0	Meteorological Research Institute, Japan	1.1° × 1.1°	Yukimoto *et al.* [23]
	MIROC6	Japan Agency for Marine-Earth Science and Technology (JAMSTEC), Kanagawa	1.4063° × 1.4063°	Tatebe & Watanabe [24]
	CMCC-CM2-SR5	Fondazione Centro Euro-Mediterraneo sui Cambiamenti Climatici, Lecce Italy	1.25° × 0.9375°	Lovato & Peano [25]
	IPSL-CM6A-LR	Institute Pierre Simon Laplace, Paris	2.5° × 2.5°	Boucher *et al.* [26]

These GCMs were selected based on performance assessments from numerous studies using various statistical measures. Boucher *et al.* [26] and Salehie *et al.* [27] reported that climate uncertainty is projected to increase towards the end of the century, driven by SSPs. According to Shiru & Chung [28], CMCC-CM2-SR5 and IPSL-CM6A-LR ranked highest for precipitation projection, while MRI-ESM2-0 and MIROC6 ranked highest for projected maximum and minimum temperatures, respectively, compared to 10 other global climate models. Furthermore, Iqbal *et al.* [22] and Wang *et al.* [29] supported the suitability of MRI-ESM2-0 as the most reliable GCM for rainfall projection in Asia. For the analysis, this study employed the multi-model ensemble of the selected GCM outputs derived from the first realisation ('r1i1p1f1'), for both the historical experiments, and future medium and high emission scenarios (SSP2–4.5 and SSP5–8.5). For analysing the future rainfall, the future periods are segmented into 30 years' time period 2025–2050 and 2051–2100 relative to the reference period (1985–2014).

In the study, the ensemble mean was selected as a straightforward and widely used method to aggregate climate model projections, providing a central estimate that reflects the average behavior of the ensemble. This approach is commonly employed in climate modeling studies, as it offers simplicity and transparency in presenting multi-model outputs. However, it is important to acknowledge its limitations, including the potential for overemphasizing models with systematic biases and the inability to account for model performance variability. Alternative methods, such as the median, Reliability Ensemble Averaging (REA), or skill-weighted averaging, may offer advantages in reducing the influence of outliers and incorporating model reliability. These methods have been discussed in the literature [30], [31] and could be considered in future analyses to enhance the robustness of ensemble projections.

2.4 Bias Correction Using Linear Scaling Model

The statistical downscaled future climate change data required a bias correction to remove the biases between the downscaled with the observed data. In this study, linear scaling model was used. The bias correction was carried out using the historical dataset generated from the downscaled GCMs model and the observed data from the selected ground stations. This results in more consistent values with the observation over the historical period. The bias correction was applied on each of the 12 months temperature data with separate calibration for each station. The linear scaling model equation is given as follows.

$$BC = \frac{P_{obs(avg)}}{P_{sim(avg)}} \tag{2}$$

where P_{obs} refers to average of monthly rainfall observed data, P_{sim} refers to average of monthly rainfall data from CMCC-CM2, IPSL-CM6A, MIROC6 and MRI-ESM2.

2.5 Rainfall Trend Analysis Using Percentile Method

The rainfall events were divided into three categories: very wet (90th percentile as P90), moderate (50th percentile as P50), and very dry (10th percentile as P10) to assess potential changes in the frequency of rainfall frequency. Daily rainfall data for the 76-year record (2025-2100) with magnitudes ≥1 mm was used to construct these long-term percentiles. This analysis considered only the projected outputs from four GCMs model under AR6 to represent the latest projected rainfall trend analysis. The percentile thresholds were determined by cumulating the projected daily rainfall values and identifying the corresponding percentile levels (P10, P50, and P90). The rainfall frequencies at each significant level were then determined by considering all forecasted GCMs data. Finally, the effective rainfall was determined by subtracting the rainfall amount of the preceding and following days. Percentile-based thresholds have been widely used to assess changes in rainfall extremes [32], while internationally recognized standards such as the Expert Team on Climate Change Detection and Indices (ETCCDI) recommend the use of defined indices including R95p, RX1day, CDD, and PRCPTOT, to characterize precipitation extremes [33].

3. Results and Discussion

3.1 Future Changes of Rainfall

The CMCC-CM2, IPSL-CM6A, MIROC6 and MRI-ESM2 models adopted the SSPs scenarios were used to examine potential future changes of rainfall characteristics over the Padas River Basin. The changes were computed for two future time slices (2025–2050 and 2051–2100) relative to the reference period (1985–2014) under two (2) SSPs (SSP2–4.5 and SSP5–8.5). The further analysis was proceeded which to analyse the climate – bias correction analyses process. After the bias correction was applied to the downscaled data from GCMs, the performances of the CMCC-CM2, IPSL-CM6A, MIROC6 and MRI-ESM2 were first examined and plotted as shown in Fig. 3. This figure compares the monthly rainfall between the historical (1985–2014) and the simulated GCMs ensembles. In this study, the GCMs were compared based on average of 30 years length of records data. It is noted that the simulated rainfall and patterns generally resemble those in the historical observations with a minimum of 5% inaccuracy. For calculating the changes in monthly simulated rainfall, the projected values were compared with the annual average rainfall for the historical period. According to the result, the change was found to range from -6.41 to 3.56%.

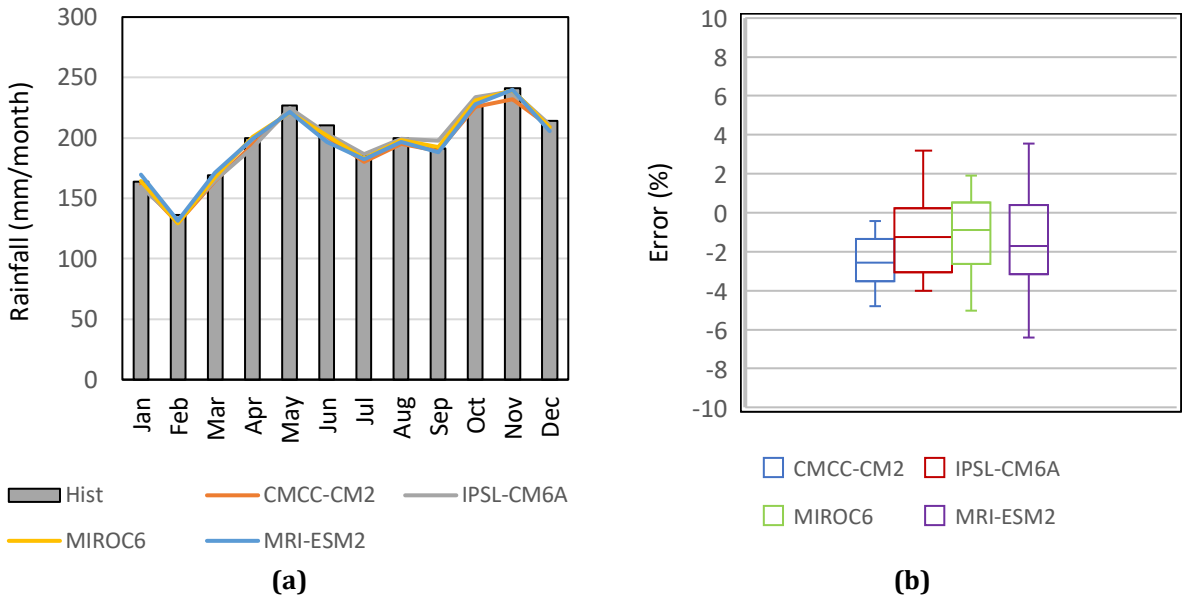

Fig. 3 *(a) Comparison of monthly rainfall (1985-2014) between historical and simulated GCMs from AR6; (b) Error (in percentage) of monthly rainfall between historical and simulated GCMs from AR6*

3.2 Climate Projection

The projection for both SSPs considers two time periods: 2025–2050 (near future) and 2051–2100 (far future) relative to a baseline period so as to compare changes in the near future and towards the end of the century as shown in Fig. 4. For the 2025–2050 period, generally, the projection using the AR6 models was found to be more

Int. Journal of Integrated Engineering Vol. 17 No. 9 (2025) p. 420-433

consistent with the historical observations. The projected annual rainfall ranged from 2302 to 2692 mm. While the increase during the period 2025 – 2051 is not particularly drastic, the projected increase for the period 2051–2100 is very significant. The projection results suggested increasing rainfall for all months in the future which can be attributable to lengthen wet season during the period. In comparison to the historical period, the changes in the long-term mean monthly rainfall ranged from 5.52 to 60.28 mm. The change in monthly rainfall from May to November could lead to higher flood risk.

Meanwhile Fig. 5 shows the changes in the long-term mean monthly rainfall for SSP2-4.5 and SSP5-8.5 within the ranged from -1.3 % to 13.2 %. Each SSPs produces different changes pattern due to different GHGs effect. However, all SSPs agreed the increase in rainfall was expected for all months in the future except in December under SSP2-4.5. The highest change in monthly rainfall was projected to be in July (2025-2050) and Sept (2051-2100). According to the result, it clearly showed that the SSP5-8.5 produces greater percentage of rainfall changes (+increment). With consistent rainfall pattern in the future year, however the rainfall intensity was expected to rise especially during North-East Monsoon.

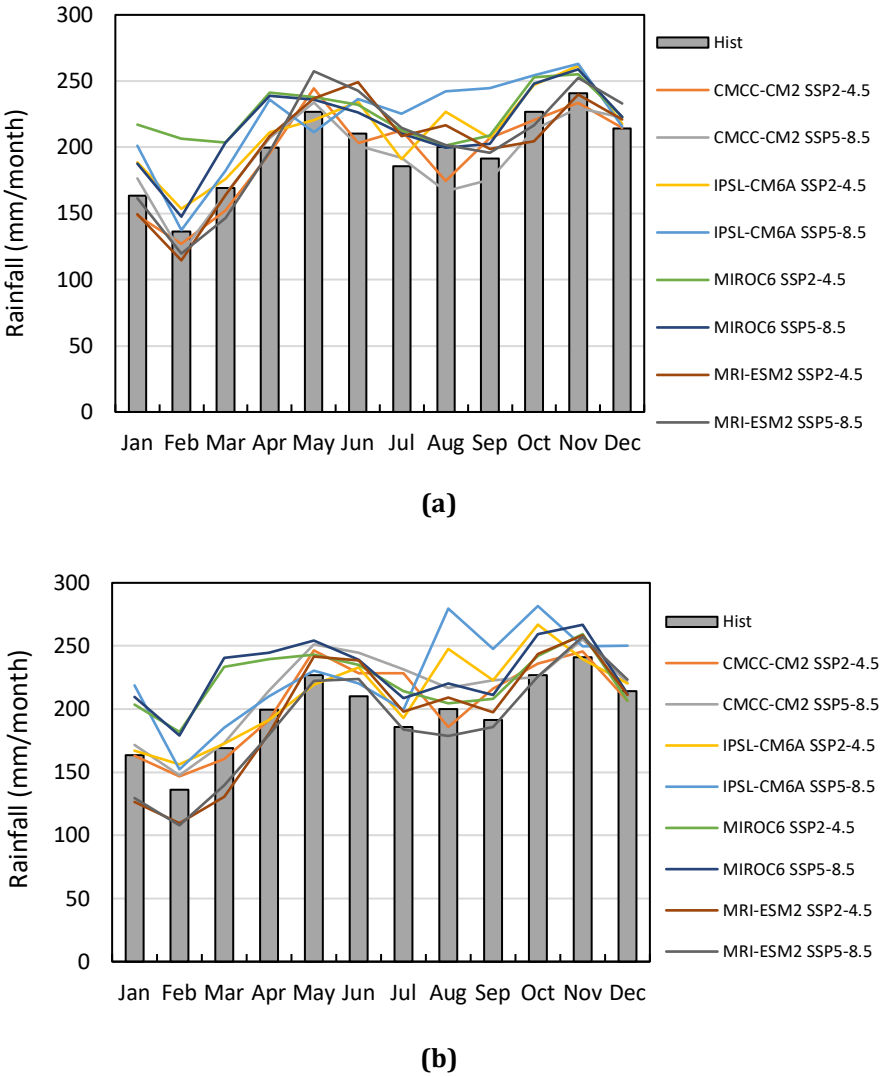

Fig. 4 *Comparison of projected monthly rainfall (a) 2025–2050; (b) 2051–2100*

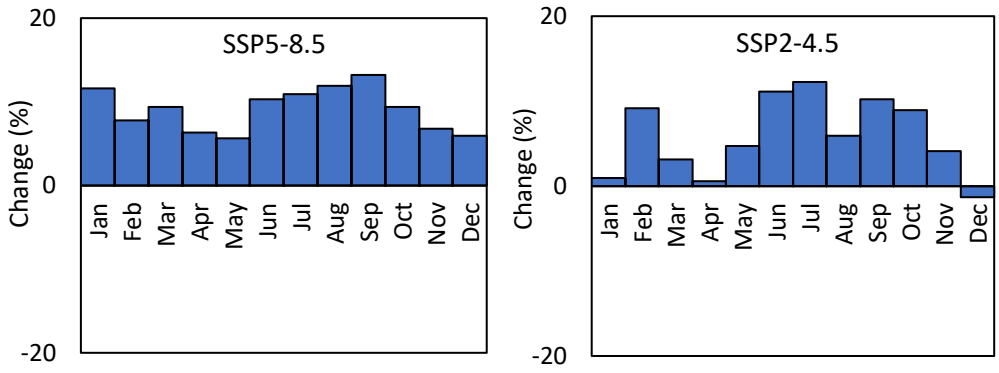

Fig. 5 *Monthly rainfall changes (in percentage) by AR6 (CMCC-CM2, IPSL-CM6A, MRI-ESM2 & MIROC6) in Δ2080*

To visualize the spatial variations of the annual rainfall for 2025–2100, the projected values from the models and SSPs are mapped using the geographic information system (GIS) as shown in Fig. 6. In this study, kriging method was applied. This technique is widely used to interpolate between low and high rainfalls. The colour scales for the maximum and the minimum values for each of the plots are fixed for comparison purposes. The values show considerable spatial variations. As summary, all models projected similar pattern of rainfall with the northeast part of the basin will receive more rainfall. Under SSP2–4.5, the IPSL-CM6A and MIROC6 projected higher rainfall compared to CMCC-CM2 and MRI-ESM2. Meanwhile for SSP5–8.5, the IPSL-CM6A was projected to receive more rainfall especially at the northeast part of the basin but MRI-ESM2 projected lower rainfall in the future compared to the other models.

The mean annual rainfall was predicted to increase in the future under SSP2–4.5 scenario. The projected annual rainfall ranges from 1824 to 2998 mm for CMCC-CM2, from 1771 to 3111 mm for IPSL-CM6A, from 1607 to 2918 mm for MRI–ESM2 and from 1765 to 3769 mm for MIROC6. The average ranges from 2121 to 3010 mm. For SSP5–8.5, the average annual rainfall was found to be slightly lower, with values ranging from 2061 to 2904 mm. It is worth to mention that the results and interpretation of downscaling climate change projection is subjected to uncertainties associated with GCMs used and pathways scenarios considered. These spatial trends are consistent with the findings of Zulfaqar *et al.* [6] and Pour *et al.* [21], who observed similar increases in rainfall over Borneo and Peninsular Malaysia, respectively, under CMIP6 projections. Liang *et al.* [16] also noted that enhanced Borneo vortex activity contributes to intensified local convection and heavy rainfall along the island's western coast, including parts of the Padas Basin. The spatial rainfall pattern identified in this study therefore reflects both large-scale atmospheric circulation changes and local topographic controls.

Table 3 presents the minimum and maximum projected annual rainfall for the near future (2025–2050) and far future (2051–2100). Overall, all four GCMs indicate an increasing trend in annual rainfall across both emission pathways, with higher values under the high-emission scenario (SSP5–8.5). The MIROC6 model projects the highest rainfall (up to 3,768.7 mm under SSP2–4.5 and 3,451.8 mm under SSP5–8.5), while MRI-ESM2 predicts the lowest (around 1,607.1–1,748.3 mm). The broader range of rainfall under SSP5–8.5 reflects greater inter-model variability, likely due to stronger greenhouse gas forcing and enhanced atmospheric moisture capacity. These findings suggest that future climate conditions will generally be wetter, particularly toward the end of the century, implying higher runoff potential and increased flood risk in low-lying and coastal areas of the basin.

Int. Journal of Integrated Engineering Vol. 17 No. 9 (2025) p. 420-433

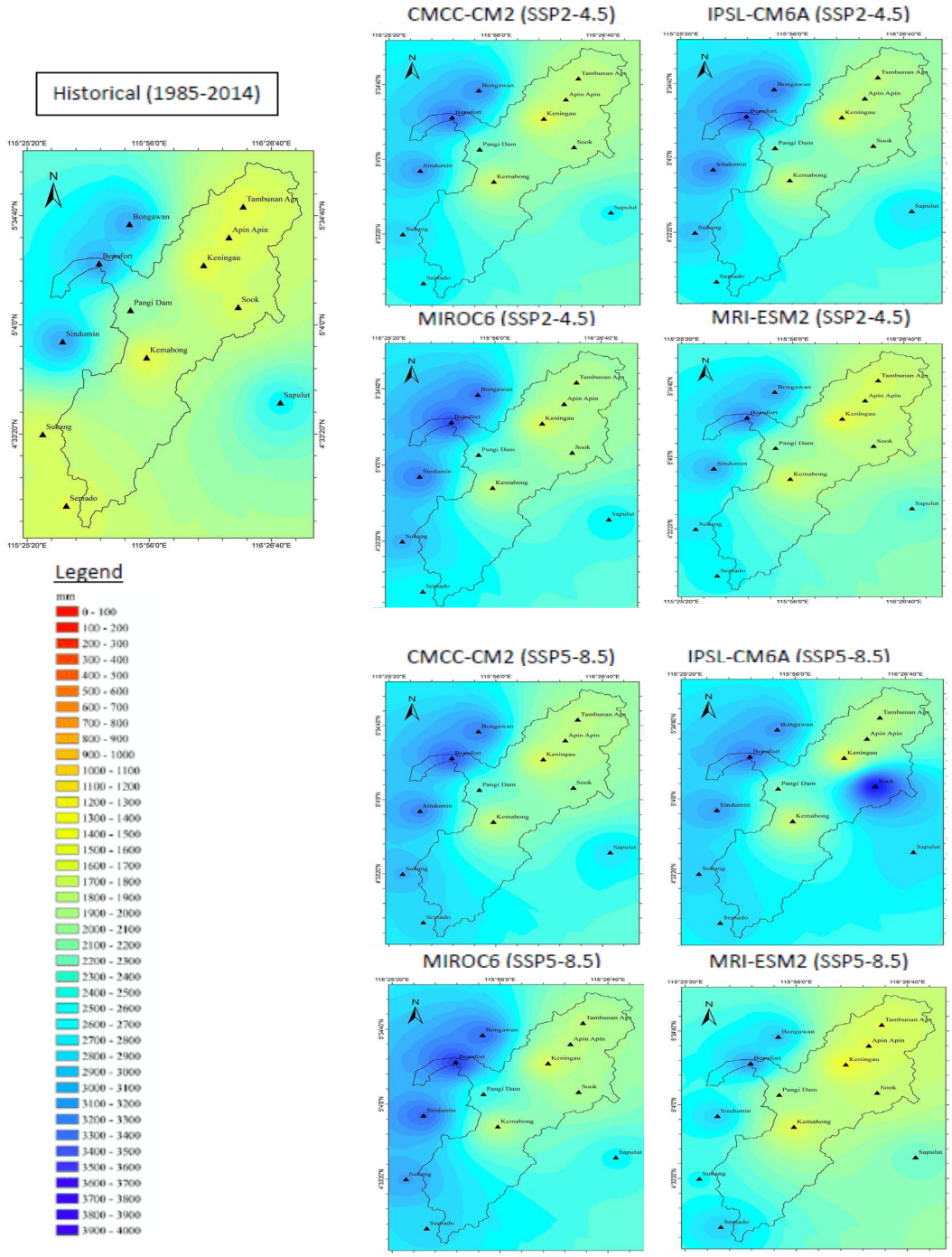

Fig. 6 *Spatial projected rainfall (2050 to 2100) by SSP2-4.5 and SSP5-8.5*

Table 3 *Minimum and maximum annual rainfall by SSP2-4.5 and SSP5-8.5*

GCMs	SSP2-4.5				SSP5-8.5			
	2025-2050		2051-2100		2025-2050		2051-2100	
	Min	Max	Min	Max	Min	Max	Min	Max
IPSL-CM6A	2069.5	2939.6	1771.5	3111.4	2080.3	3330.8	2140.0	3466.0
CMCC-CM2	1559.5	2875.6	1823.9	2997.8	1476.2	3182.4	1882.4	3241.4
MIROC6	1768.0	3516.5	1765.3	3768.7	1865.8	3326.6	1882.1	3451.8
MRI-ESM2	1748.9	2914.8	1607.1	2917.7	1999.1	3106.6	1748.3	2953.4

3.3 Rainfall Trend Analysis Using Percentile

Fig. 7 illustrates the cumulative projected rainfall for 10th (P10), 50th (P50) and 90th (P90) percentiles for one of the stations. Meanwhile Fig. 8 indicates the monthly rainfall ranges accordance to percentiles for each station. Rainfall percentile is used to measure the frequency of exceedance with respect to a percentile-based threshold [19]. The P10, P50, and P90 refer to 10%, 50% and 90% chances of any rainfall amount being equal to or below that particular value, respectively. It is important to analyze using percentile indices because there is variation in the potential rainfall that provided by four (4) different GCMs. Furthermore, the analyses are carried out the impact on the water resources within Padas River Basin for different long-term projection scenarios (10th, 50th and 90th percentile rainfall).

The comparison of effective rainfall by considering from 12 rainfall stations were carried out. Based on rainfall percentile results, all stations showed consistent rainfall trend except at Stn Sook (5163002). The gap between P90 and P50 was rather large. It will be impacted by the IPSL projection in this area, which predicts large changes in future years. The gap between P50 and P90 is 300 mm/month. Besides, there are three (3) stations that producing higher long-term P90 (<300,000 mm of cumulative rainfall projection until 2100) such as Stn. Bongawan (5558001), Stn. Sindumin (4955001) and Stn. Beaufort (5357003). These stations are located near to the coastal area making these areas receive higher rainfall than other parts of the Padas River Basin. These areas are particularly sensitive to increased monsoonal intensity and convective rainfall driven by warmer sea-surface temperatures. Similar coastal amplification effects were reported by Adib *et al.* [34] and Tan *et al.* [20] for other Malaysian basins.

Meanwhile based on monthly rainfall, the maximum P90 is potentially to occur with less than 1000 mm/month in April and Jan at certain areas in this river basin. The high rainfall intensity is projected under by SSP5-8.5 that receiving high climate change impacts.

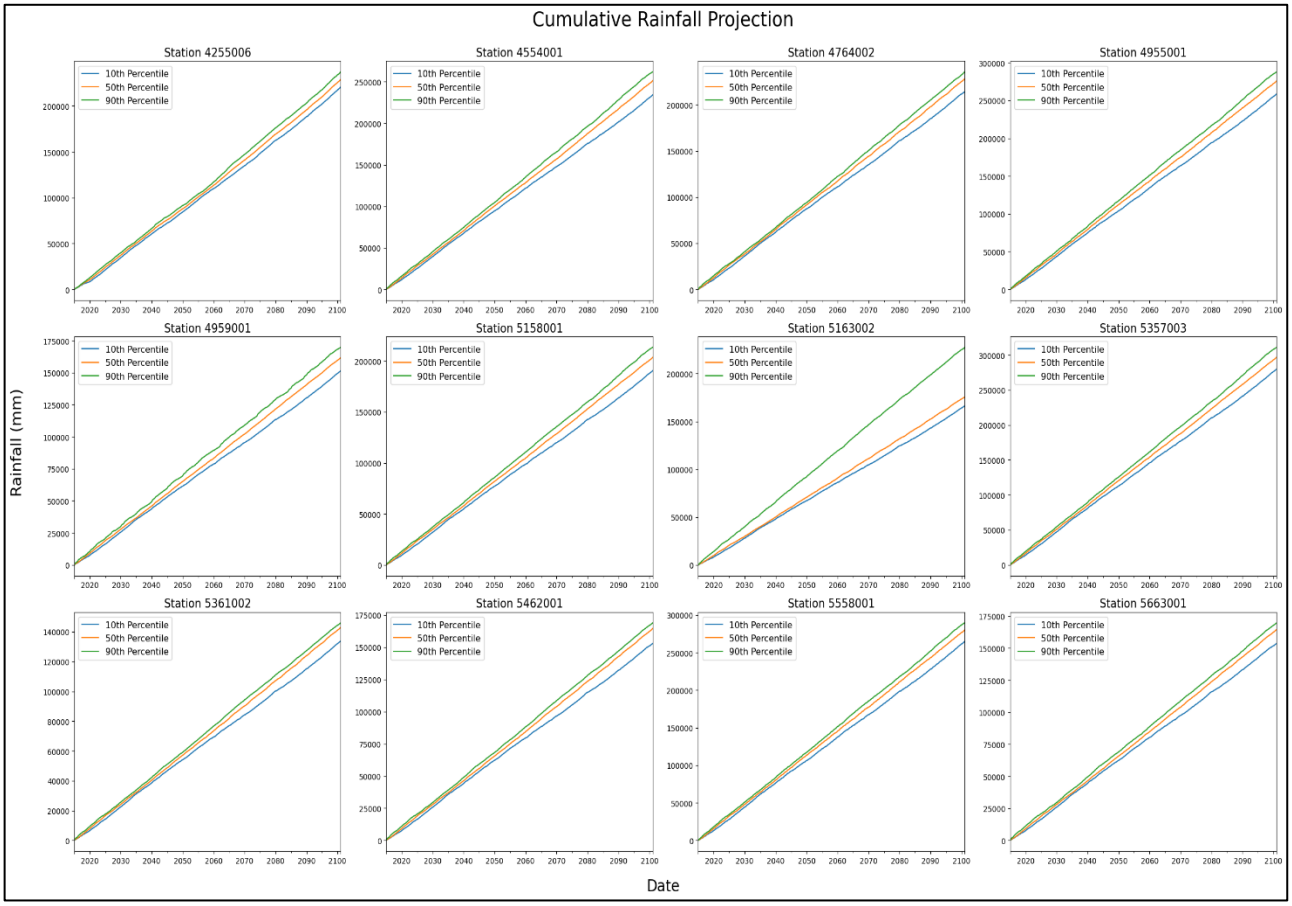

Fig. 7 *Annual cumulative rainfall for 10th, 50th and 90th percentile based on 2020-2100*

Int. Journal of Integrated Engineering Vol. 17 No. 9 (2025) p. 420-433

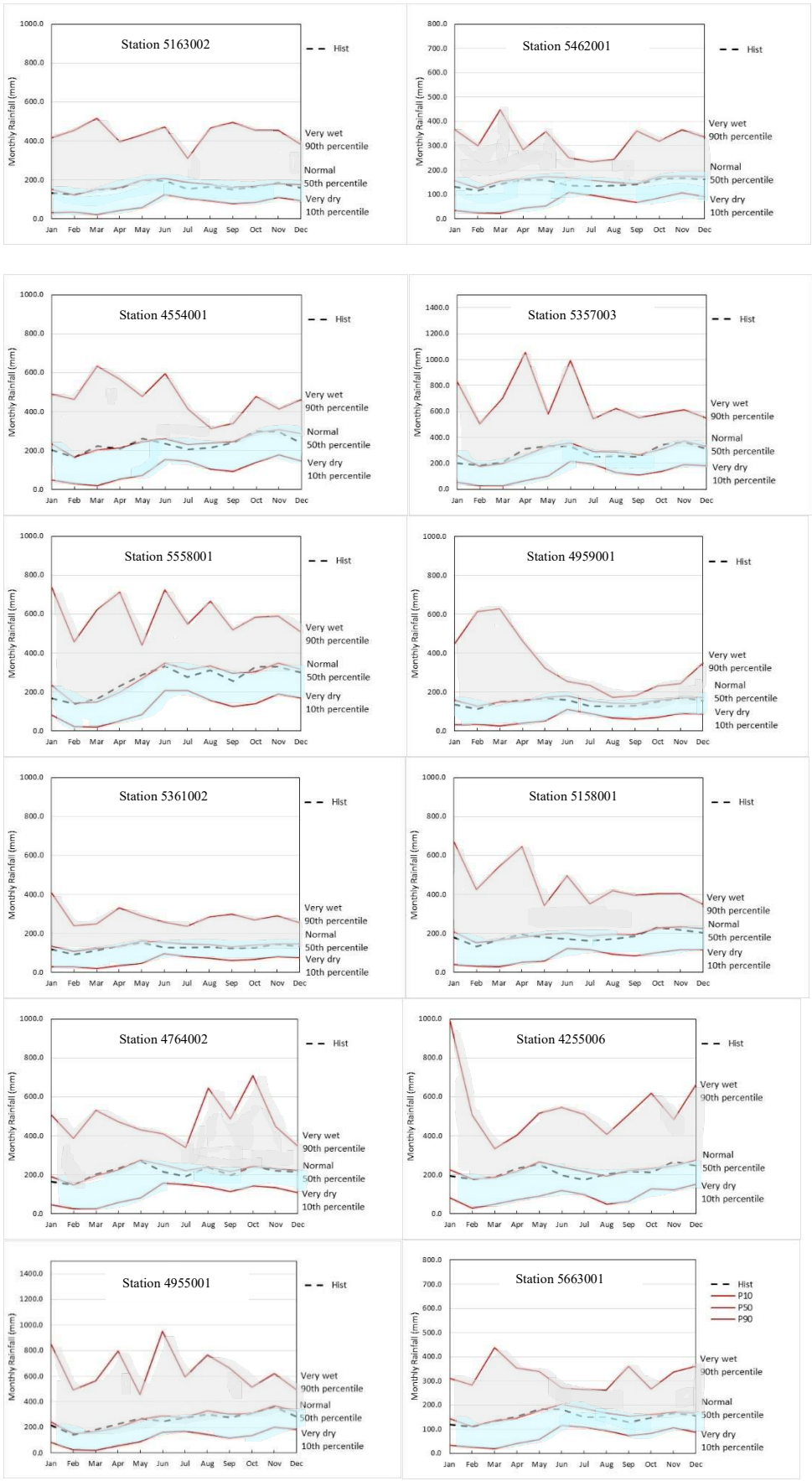

Fig. 8 *Monthly cumulative rainfall for 10th, 50th and 90th percentile based on 2020-2100 (White: P10 (very dry); Light Blue: P50 (moderate); Grey: P90 (very wet))*

4. Conclusions

The climate change phenomenon brings significant effects to the long-term climate pattern. Hence, it is important to study the impact of climate change on the variation of climate variables, especially in a river basin. In the current study, Padas River basin in Sabah was chosen due to its significant for water supply and irrigation. This study simulated the climate projection by using historical rainfall data from 1985 to 2014. The simulated rainfall pattern generally resembles those in the historical observations. The results indicate that annual rainfall is expected to rise by approximately 5.4% (2025–2050) and 7.4% (2051–2100), with the highest intensity focused near the coastal areas. The greatest monthly increase is projected in May (+60.3 mm) followed by November (+46.8 mm), while February shows the least increment (+5.5%). SSP5–8.5 projects the highest overall increase, with average annual rainfall reaching 4,030 mm during 2051–2100, compared to 3,625 mm under SSP2–4.5. Among the models. MRI-ESM2 projected the least rainfall changes (+1.1%) in future rainfall. Keningau, Tambunan, Apin-apin and Kemabong areas are expected to receive relatively lower rainfall. The percentile analysis revealed that coastal areas will be more exposed to higher cumulative rainfall (P90 < 300,000 mm within 76 years), suggesting increased flood potential, while the long-term P50 results align closely with historical monthly trends.

Although this study provides important insights into projected rainfall changes over the Padas River Basin, the results should be interpreted with consideration of model-related uncertainties. The variation among GCMs indicates a noticeable inter-model spread, particularly under the high-emission scenario, reflecting the sensitivity of rainfall projections to model physics and greenhouse gas forcings. Future studies should incorporate multiple realizations and standardized extreme indices to enhance the robustness of projections and provide a more comprehensive uncertainty analysis. From a policy perspective, the projected increase in rainfall and wet-season intensification underscores the need for adaptive water management strategies, flood mitigation measures, and integration of climate projections into basin-scale planning and climate-resilient water governance in Sabah.

Acknowledgement

The authors would like to thank the government of Malaysia through its implementing agency, the Department of Irrigation and Drainage (DID/JPS) for providing the information required to conduct this work.

Conflict of Interest

Authors declare that there is no conflict of interests regarding the publication of the paper.

Author Contribution

The authors confirm contribution to the paper as follows: ***study conception and design:*** *Siti Nazahiyah, Nurul Nadrah, Muhammad Syukri, Foo Hoat Lim;* ***data collection:*** *Ahmad Safiuddin, Muhammad Hanafi;* ***analysis and interpretation of results:*** *Siti Nazahiyah, Nurul Nadrah;* ***draft manuscript preparation:*** *Siti Nazahiyah, Nurul Nadrah. All authors reviewed the results and approved the final version of the manuscript.*

References

[1] Nakicenovic, N., Alcamo J, Grubler, A. *et al* (2000) Special report on emissions scenarios (SRES), a special report of working group III of the intergovernmental panel on climate change. Cambridge University Press, Cambridge.

[2] IPCC (2013) Climate change 2013: the physical science basis. Contribution of working group I to the fifth assessment report of the intergovernmental panel on climate change. Cambridge University Press, Cambridge.

[3] Riahi, K., van Vuuren, D. P., Kriegler, E., Edmonds, J., O'Neill, B. C., Fujimori, S., Bauer, N., Calvin, K., Dellink, R., Fricko, O., Lutz, W., Popp, A., Cuaresma, J. C., KC, S., Leimbach, M., Jiang, L., Kram, T., Rao, S., Emmerling, J., … Tavoni, M. (2017) The Shared Socioeconomic Pathways and their energy, land use, and greenhouse gas emissions implications: An overview, *Global Environmental Change*, *42*, 153–168, https://doi.org/10.1016/j.gloenvcha.2016.05.009

[4] Tang K. H. D. (2019) Climate change in Malaysia: trends, contributors, impacts, mitigation and adaptations, *Sci Total Environ*, *650 (Part 2)*, 1858–1871, https://doi.org/10.1016/j.scitotenv.2018.09.316

[5] Mohseni, U., Agnihotri, P. G., Pande, C. B. & Durin, B. (2023) Understanding the climate change and land use impact on streamflow in the present and future under CMIP6 climate scenarios for the Parvara Mula basin, India, *Water*, *15(9)*, 1753, https://doi.org/10.3390/w15091753

[6] Zulfaqar Sa'adi, Z., Al-Suwaiyan, M. S., Yaseen, Z. M., Tan, M. L., Goliatt, L., Heddam, S., Halder, B., Ahmadianfar, I., Homod, R. Z. & Shafik, S. S. (2024) Observed and future shifts in climate zone of Borneo based on CMIP6 models, *Journal of Environmental Management*, *360*, 121087, https://doi.org/10.1016/j.jenvman.2024.121087

[7] Wang, J-xia, Huang, J-kun, & Yan, T-ting. (2013) Impacts of climate change on water and agricultural production in ten large river basins in China, *Journal of Integrative Agriculture*, *12(7)*, 1267–1278, https://doi.org/10.1016/S2095-3119(13)60421-9

[8] Uniyal, B., Jha, M. K., & Verma, A. K. (2015) Assessing climate change impact on water balance components of a river basin using SWAT model, *Water Resources Management*, *29(13)*, 4767–4785, https://doi.org/10.1007/s11269-015-1089-5

[9] Huang, W.-R., Chang, Y.-H. & Liu, P.-Y. (2018) Assessment of IMERG precipitation over Taiwan at multiple timescales, *Atmos. Res.*, *214*, 239–249, https://doi.org/10.1016/j.atmosres.2018.08.004

[10] Umar, D. A., Ramli, M. F., Aris, A. Z., Jamil, N. R. & Aderemi, A. A. (2019) Evidence of climate variability from rainfall and temperature fluctuations in semi-arid region of the tropics, *Atmospheric Research*, *224*, 52-64, https://doi.org/10.1016/j.atmosres.2019.03.023

[11] Khan, N, Pour, S. H., Shahid, S., Ismail, T., Ahmed, K., Chung, E. S., Nawaz, N. & Wang, X. (2019) Spatial distribution of secular trends in rainfall indices of Peninsular Malaysia in the presence of long-term persistence, *Meteorol Appl.*, *26*, 655– 670, https://doi.org/10.1002/met.1792

[12] Karki, R., ul Hasson, S., Gerlitz, L., Talchabhadel, R., Schenk, E., Schickhoff, U., Scholten, T. & Böhner, J. (2020), Rising mean and extreme near-surface air temperature across Nepal, *Int. J. of Climatology*, *40(4)*, 2445-2463, https://doi.org/10.1002/joc.6344

[13] Adib M. N. M., Rowshon, M. K., Mojid, M. A., Habibu, I. (2020) Projected streamflow in the Kurau River Basin of Western Malaysia under future climate scenarios, *Sci Rep*, *10*, 8336, https://doi.org/10.1038/s41598-020-65114-w

[14] Hamed, M. M., Al-Sakkaf, A. S., Rady, M. & Shahid, S. (2024) Temperature and precipitation extremes over Borneo Island: an integrated climate risk assessment, *International Journal of Climatology*, *44(16)*, 6040-6064, https://doi.org/0.1002/joc.8682

[15] Sa'adi, Z., Shahid, S., Chung, E-S. & Ismail, T (2017) Projection of spatial and temporal changes of rainfall in Sarawak of Borneo Island using statistical downscaling of CMIP5 models, *Atmospheric Research*, 197, 446-460, https://doi.org/10.1016/j.atmosres.2017.08.002

[16] Liang, J., Catto, J. L., Hawcroft, M. K. (2023) Borneo vortices in a warmer climate, *npj Clim Atmos Sci*, *6*, 2, https://doi.org/10.1038/s41612-023-00326-1

[17] Yu, X., Zhang, L., Zhou, T. & Zheng, J. (2024) Assessing the performance of CMIP6 models in simulating droughts across global drylands, *Adv. Atmos. Sci*. *41*, 193–208, https://doi.org/10.1007/s00376-023-2278-4

[18] Riahi, K., van Vuuren, D. P., Kriegler, E., Edmonds, J., O'Neill, B. C., Fujimori, S., Bauer, N., Calvin, K., Dellink, R., Fricko, O., Lutz, W., Popp, A., Cuaresma, J. C., Kc, S., Leimbach, M., Jiang, L., Kram, T., Rao, S., Emmerling, J., Eom, J., … Tavoni, M. (2017) The shared socioeconomic pathways and their energy, land use, and greenhouse gas emissions implications: An overview, *Global Environmental Change*, *42*, 153–168, https://doi.org/10.1016/j.gloenvcha.2016.05.009

[19] Teegavarapu, R. S. V. & Chandramouli, V. (2005) Improved weighting methods, deterministic and stochastic data-driven models for estimation of missing precipitation records, *Journal of Hydrology*, *312(1–4)*, 191–206, https://doi.org/10.1016/j.jhydrol.2005.02.015

[20] Tan, M. L., Liang, J., Samat, N., Chan, N. W., Haywood, J. M. & Hodges, K. (2021) Hydrological extremes and responses to climate change in the Kelantan River Basin, Malaysia, based on the CMIP6 HighResMIP experiments, *Water (Switzerland)*, *13(11)*, 1472, https://doi.org/10.3390/w13111472

[21] Pour, S. H., Shahid, S. & Mainuddin, M (2022) Relative performance of CMIP5 and CMIP6 models in simulating rainfall in Peninsular Malaysia, *Theoretical and Applied Climatology*, *149*, 709–725, https://doi.org/10.1007/s00704-022-04076-7

[22] Iqbal, Z., Shahid, S., Ahmed, K., Ismail, T., Ziarh, G. F., Chung, E-S. (2021) Evaluation of CMIP6 GCM rainfall in mainland Southeast Asia, *Atmospheric Research*, *254(1)*, 105525, https://doi.org/10.1016/j.atmosres.2021.105525

[23] Yukimoto, S., Koshiro, T., Kawai, H., Oshima, N., Yoshida, K., Urakawa, S., Tsujino, H., Deushi, M., Tanaka, T. & Hosaka, M. (2019) MRI MRI-ESM2.0 model output prepared for CMIP6 CMIP historical, Version 20190222; Earth System Grid Federation: Washington, DC, USA.

[24] Tatebe, H. & Watanabe, M. (2018) MIROC6 model output prepared for CMIP6 CMIP historical, Version 20181212; Earth System Grid Federation: Washington, DC, USA.

[25] Lovato, T. & Peano, D. (2020) IPCC DDC: CMCC CMCC-CM2-SR5 model output prepared for CMIP6 CMIP historical, World Data Center for Climate (WDCC) at DKRZ, https://doi.org/10.26050/WDCC/AR6.C6CMCMCCShi

[26] Boucher, O., Denvil, S., Levavasseur, G., Cozic, A., Caubel, A., Foujols, M.A., Meurdesoif, Y., Cadule, P., Devilliers, M. & Ghattas, J. (2018) IPSL IPSL-CM6A-LR model output prepared for CMIP6 CMIP historical, Version 20180803; Earth System Grid Federation: Washington, DC, USA, 2018.

[27] Salehie, O., Hamed, M. M., Ismail, T., Tam, T. H. & Shahid, S. (2021) Selection of CMIP6 GCM with projection of climate over the Anu Darya River Basin, *Theor Appl Climatol*., *151,* 1185–1203, https://doi.org/10.1007/s00704-022-04332-w

[28] Shiru, M. S. & Chung, E-S. (2021) Performance evaluation of CMIP6 global climate models for selecting models for climate projection over Nigeria, *Theoretical and Applied Climatology*, *146 (1)*, 599-615, https://doi.org/10.1007/s00704-021-03746-2

[29] Wang, L., Zhang, J-Y., Shu, Z., Wang, Y., Bao, Z., Liu, C., Zhou, X. & Wang, G. (2021) Evaluation of the ability of CMIP6 global climate models to simulate precipitation in the Yellow River Basin, China, *Frontier in Earth Science*, *9*, 751974, https://doi.org/10.3389/feart.2021.751974

[30] Knutti, R., Furrer, R., Tebaldi, C., Cermak, J. & Meehl, G. A. (2010) Challenges in combining projections from multiple climate models, *Journal of Climate*, *23(10)*, 2739-2758, https://doi.org/10.1175/2009JCLI3361.1

[31] Herger, N., Abramowitz, G., Knutti, Angélil, O., Lehmann, K. & Sanderson, B. M. (2018) Selecting a climate model subset to optimise key ensemble properties, *Earth System Dynamics*, *9(1)*, 135–151, https://doi.org/10.5194/esd-9-135-2018

[32] Schär, C., Ban, N., Fischer, E. M., Rajczak, J., Schmidli, J., Frei, C., Giorgi, F., Karl, T. R., Kendon, E. J., Tank, A. M. G. K., O'Gorman, P. A., Sillmann, J., Zhang, X. & Zwiers, F. W. (2016) Percentile indices for assessing changes in heavy precipitation events, *Climatic Change*, *137*, 201–216, https://doi.org/10.1007/s10584-016-1669-2

[33] Zhang, X., Alexander, L., Hegerl, G. C., Jones, P., Tank, A. K., Peterson, T. C., Trewin, B. & Zwiers, F. W. (2011) Indices for monitoring changes in extremes based on daily temperature and precipitation data, *WIREs Climate Change*, *2(6)*, 851–870, https://doi.org/10.1002/wcc.147

[34] Mohd Adib, M. N., Harun, S. & Rowshon, M. K. (2022) Long-term rainfall projection based on CMIP6 scenarios for Kurau River Basin of rice-growing irrigation scheme, Malaysia, *SN Appl. Sci*, *4(70)*, https://doi.org/10.1007/s42452-022-04952-x